

Influence of Pool Size and Fuel Type on the Liquid Fuel Temperature Profile during Burning of Pool Fires in Open Atmosphere

Pretrél H.

*Institut de Radioprotection et de Sûreté Nucléaire (IRSN), PSN-RES, SA2I,
Centre de Cadarache, St Paul Lez Durance, France
Email: hugues.pretrél@irsn.fr*

ABSTRACT

This study aims at better understanding the heat and mass transfer processes at the liquid fuel surface during a pool fire. It proposes new experimental data regarding the characteristics of the vertical temperature profile in the vicinity of the fuel surface in both liquid and gas phases. This analysis is based on pool fire experiments in open atmosphere, performed with various pool sizes from 0.1 m² to 1 m², and for four different fuels: ethanol, dodecane, hydrogenated tetra propylene (or HTP) and lubricant oil. The vertical temperature profiles are obtained from the measurements of the temperature within the pool and of the fuel mass loss rate. For ethanol, dodecane and HTP fuels, the temperature profile shows a thin upper layer of about 4 mm in the liquid fuel at constant temperature equal to the boiling one. For lubricant oil fuel, no constant temperature upper layer is observed. In addition, the temperature profiles allow characterizing the convective heat transfer in the gas phase through the determination of the temperature gradient. These measurements propose valuable information for the validation of fuel evaporation models, used for the numerical prediction of pool fires.

KEYWORDS: Pool fire, liquid fuel, pyrolysis, temperature profile.

INTRODUCTION

The understanding of the heat and mass transfer processes at a liquid fuel surface remains a key issue in the prediction of the burning rate of pool fires. Fuel vaporization leading to the process of burning results from the heat energy balance through the fuel layer [1]. The heat fluxes involved in this process are illustrated in Fig. 1.

The two dominant heat sources contributing to the evaporation process are the incident radiative heat flux coming from the flame (Rad.) and the convective heat transfer at the fuel surface heating the fuel layer (Conv.). Additional terms modulating the effects of the two former contributions are the reflection of the incident radiation heat flux (Refl.), the radiative emission of the fuel surface (Emit.), the heat flux transferred by conduction by the pan to the liquid fuel (Cond.), the thermal losses (Loss) and the latent heat required to heat up the mass of fuel. The net balance of all these contributions equals the energy for evaporating the mass of fuel. This thermal process leads to a specific temperature field within the fuel layer and the gas phase. This profile is mainly one-dimensional in the vertical direction as illustrated in Fig. 1.

Research studies on pool fires have been numerous over several decades and have led to a deep understanding of such fires based mainly on a wide range of experimental approaches [2-4]. More recently, numerical simulations using computational fluid dynamic (CFD) approaches have been proposed with very encouraging results [5-7]. An important issue from these simulations is the

Proceedings of the Ninth International Seminar on Fire and Explosion Hazards (ISFEH9), pp. 662-671

Edited by Snegirev A., Liu N.A., Tamanini F., Bradley D., Molkov V., and Chaumeix N.

Published by St. Petersburg Polytechnic University Press

ISBN: 978-5-7422-6496-5 DOI: 10.18720/spbpu/2/k19-48

modeling of the heat and mass transfers at the fuel surface and thus the appropriate prediction of the burning rate.

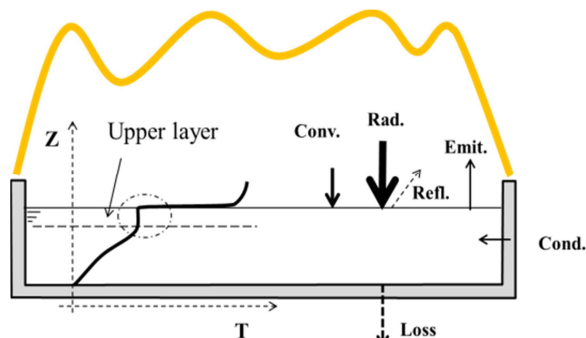


Fig. 1. Schematic illustration of the heat transfer within the liquid fuel.

Recent studies focused on this task in order to highlight the influence of boundary conditions on the burning rate with the final goal to better identify the relative contributions of each heat transfer mechanism. The pan height and the lip distance modified the convective flow within the liquid fuel [8, 9]. The pan thermal conductivity (for quartz or aluminum pan) and the liquid temperature at the bottom of the pan also influence the energy balance and thus the burning rate [4] [5]. The initial fuel height is also an important parameter and according to its value, two regimes of burning for thin and thick pool fires are identified. For thick pool regime, a uniform temperature upper layer below the fuel surface is observed with a temperature level near the boiling one and a lower layer with a nonlinear temperature gradient as illustrated in Fig. 1 [10, 11]. The occurrence of this upper layer, already identified in the 60s [12], results from the radiation heat fluxes coming from the flame and absorbed within the liquid fuel [13]. This layer is also characterized by “hot spots” on its lower side where the temperature is greater than the boiling temperature, which is evidence of a superheating process due to in-depth radiation absorption [14].

In order to improve the characterization of the heat transfer at the fuel interface, but also to propose an experimental database for the validation of fuel evaporation models, heat flux and temperature measurements remain a necessary task [15]. Recent studies have presented detailed measurements of the total heat fluxes for a gasoline 0.36 m² square pool fire [14] and vertical temperature profile for a methanol 0.1 m² circular pool fire [11]. This study presents a new set of data for the vertical temperature profile in the vicinity of the fuel interface both in the liquid and gas phases, which is barely represented in the literature. This direct measurement of the temperature profile gives information about the convective heat transfer coefficient, which is usually determined by the inverse method from the energy balance [2].

FIRE TESTS

Data come from a set of pool fire experiments performed during the international OECD PRISME project for a larger range of pool size (from 0.1 to 1 m²) and for several fuel types having different radiative properties (ethanol C₂H₆O, dodecane, hydrogenated tetrapropylene, C₁₂H₂₆ and Lubricant oil fuel, C₃₁H₆₄). Fire tests were performed in the open atmosphere SATURNE hood of IRSN at Cadarache in France (Fig. 2). Pans were metallic circular vessels of various areas from 0.10 to 1.00 m² (or in diameter from 0.35 to 1.12 m). Fuel was poured manually in the pan and then ignited by gas propane burner. The initial distance between the pool surface and the position of the burner was about 0.10 m. The pan was placed on a weighting system to measure the mass of fuel. Five K-type thermocouples of 1.5 mm diameter were positioned vertically at the center of the pan in order to characterize the temperature in the liquid fuel. These measurements will be used to determine the

vertical temperature profile in the vicinity of the fuel surface. The weighting system is accurate within 2 g and the thermocouples are verified with reference temperature and are accurate within 2°C.

Fire test characteristics are listed in Table 1. Three series of tests are considered for three fuels, hydrogenated tetrapropylene, HTP, with the chemical formulation $C_{12}H_{26}$ used as solvent in nuclear reprocessing plant, dodecane, with the same formulation $C_{12}H_{26}$ and lubricant oil DTE MEDIUM from MOBIL, $C_{31}H_{64}$. In addition, one test with ethanol fuel is considered. These fuels have different properties from light to heavier fuels as indicated in Table 2. For each series, except for the ethanol test, experiments were reproduced for repeatability or in changing initial boundary conditions (initial fuel mass, exhaust flow rate at the hood or initial fuel temperature). It has to be noted that the pan heights were different according to the test series, from 0.10 to 0.15 m.

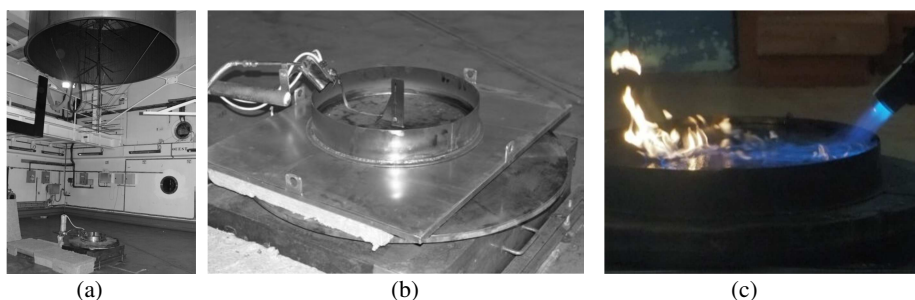


Fig. 2. Photographs of the SATURNE hood (a), of a 0.40 m² pan with the igniter (b), of the ignition phase with the 1.00 m² pan (c).

Table 1. List of experiments

Test name	Fuel type	Pool area (m ²)	Pan height (m)	Initial fuel mass (kg)
PRS_SI_S5	HTP	0.10	0.10	3.67
PRS_SI_S1	HTP	0.20	0.10	7.75
PRS_SI_S3	HTP	0.40	0.10	14.90
PRS_SI_S8	Ethanol	0.40	0.10	15.89
PR2_FESS_S11	Lub. oil	0.20	0.13	8.08
PR2_FESS_S12	Lub. oil	0.40	0.13	14.94
PR2_FESS_S13	Lub. oil	0.70	0.13	30.45
PR3_S3S_S4	Dodecane	0.10	0.15	4.19
PR3_S3S_S1	Dodecane	0.40	0.15	23.21
PR3_S3S_S2	Dodecane	0.56	0.15	28.30
PR3_S3S_S3	Dodecane	1.00	0.15	38.40

Table 2. Fuel properties

Fuel	Formulation	Density (kg/m ³) at 20°C	β Expansion coefficient (°C ⁻¹)	Boiling temperature (°C)
Ethanol	C_2H_6O	789	0.00149	78
HTP	$C_{12}H_{26}$	760	0.00124	188
Dodecane	$C_{12}H_{26}$	750	0.00120	216
Lub. oil	$C_{31}H_{64}$	870	0.00070	480

MASS LOSS RATE

Before analyzing the temperature profiles, the fuel mass loss rate (MLR) is determined and compared to literature data as a protocol validation for the fire tests. The mass loss rate is computed as the time derivative of the measured mass of fuel. The time derivative is performed with a given period of time dt such as the mass loss during this period is 20 times greater than the accuracy of the weighting system (relative uncertainty for the MLR lower than 5%). The time variations for the different fuels are given in Fig. 3 and Fig. 4. For all pool areas, the time history of the mass loss rate shows the typical behavior for such experiments with three phases: first a phase of flame propagation and fire growth, then a phase of quasi-stationary burning rate which ends with the last phase of extinction. For some tests, the extinction phase may experience peak of MLR due to the rapid evaporation of the last millimeters of fuel.

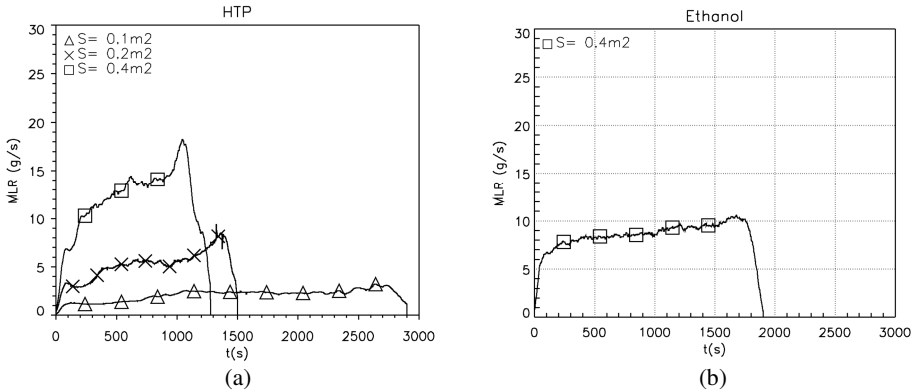


Fig. 3. Time variation of the mass loss rate for (a) HTP fuel and (b) ethanol fuel.

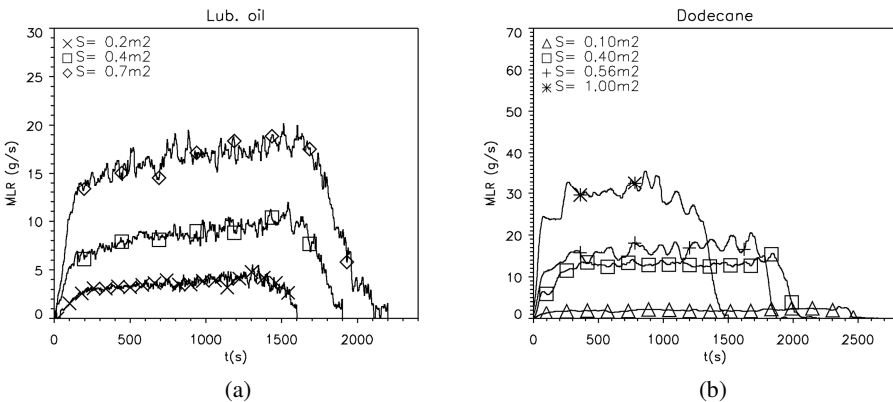


Fig. 4. Time variation of the mass loss rate for (a) lubricant oil fuel and (b) dodecane fuel.

For all tests, a time averaged mass loss rate during the steady period is computed. This mean mass loss rate divided by the pool area is plotted versus the pool diameter as indicated in Fig. 5. The variation followed with satisfactory agreement the Babrauskas’ model written as [4]:

$$\dot{m}_f'' = \dot{m}_{f,\infty}''(1 - e^{-k_\beta D}), \tag{1}$$

where \dot{m}_f'' is the mass loss rate per unit of pool area, $\dot{m}_{f,\infty}''$ is the mass loss rate per unit of pool area for large pool area, k_β is the model parameter and D the pool diameter; $\dot{m}_{f,\infty}''$ and k_β are determined

experimentally by fitting the model to the data. Their values, indicated in Fig. 5, are in good agreement with those from similar published experiments [4].

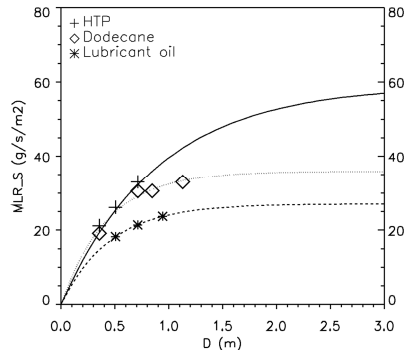


Fig. 5. Mass loss rate per unit of area versus pool diameter for HTP (with $\dot{m}_{f,\infty}'' = 59 \text{ g}/(\text{m}^2 \cdot \text{s})$ and $k_{\beta} = 1.1 \text{ m}^{-1}$), Dodecane (with $\dot{m}_{f,\infty}'' = 35 \text{ g}/(\text{m}^2 \cdot \text{s})$ and $k_{\beta} = 2.3 \text{ m}^{-1}$) and lubricant oil fuels (with $\dot{m}_{f,\infty}'' = 27 \text{ g}/(\text{m}^2 \cdot \text{s})$ and $k_{\beta} = 2.1 \text{ m}^{-1}$).

VERTICAL TEMPERATURE PROFILE

In order to investigate the vertical temperature profile within the fuel layer, thermocouples were positioned at fixed locations along a vertical axis at the center of the pan. Examples of temperature time variation given by three thermocouples are presented in Fig. 6 (a). The thermocouple being fixed, the time variation of the temperature shows a typical behavior illustrating the downward displacement of the liquid fuel surface. For each probe, three phases are observed. The first one corresponds to the temperature in the liquid phase, which increases progressively due to the heating up of the fuel as well as the reduction of the distance between the thermocouple and the fuel surface. A second phase is characterized by a plateau for which the temperature is constant and equal to the boiling temperature (here about 80°C for ethanol). This phase corresponds to the displacement of the thermocouple within a layer of liquid that remains at the boiling temperature. The third phase is characterized with a rapid rise of the temperature from the boiling temperature up to a much larger level close to the flame temperature (here about 800°C for ethanol). This last phase corresponds to the relative displacement of the thermocouple within the gas phase away from the fuel surface. This behavior of three phases is identical for the three thermocouples and is typical to such experiments [14].

To determine the vertical temperature profile, the time variation of the temperature given by a thermocouple $T(t)$ is converted into spatiale variation $T(z)$ with the following variable change. The temperature at a given time is plotted versus its relative distance to the pool surface, $z^* = z_p - z_s(t)$ expressed as the same time. This relative distance is given as the difference between the fixed position of the thermocouple, z_p , known from the experiment set up (here 4.2 cm, 3.5 cm and 2.5 cm), and the position of the fuel surface $z_s(t)$, varying with time. This position is computed with the relationship $z_s(t) = m_f(t)/[S\rho(T)]$ where $m_f(t)$, is the measured mass of fuel that varies with time, S , the constant pool area and $\rho(T)$, the liquid density which varies with the temperature and thus with time. In the present study, the liquid density is assessed from the classical thermodynamic relationship $\rho(\bar{T}_f) = \rho(T_o) \left[1 / (1 + \beta(\bar{T}_f - T_o)) \right]$ with β the volumetric expansion coefficient, T_o the ambient temperature, $\rho(T_o)$, the density at ambient temperature and \bar{T}_f , a mean temperature of the liquid fuel obtained as the average from all the thermocouples located within the fuel layer. Table 2 gives the physical properties used to compute the liquid density.

Figure 6 (a) shows an example of the time variation of the position of the fuel surface $z_s(t)$ as well as of the mean fuel temperature $\bar{T}_f(t)$. The fuel surface position decreases progressively from its initial value, here about 55 mm, toward zero indicating that all fuel is burned. The mean fuel temperature increases from the initial fuel temperature (here ambient temperature) toward the boiling temperature (dotted line in Fig. 6 (a)).

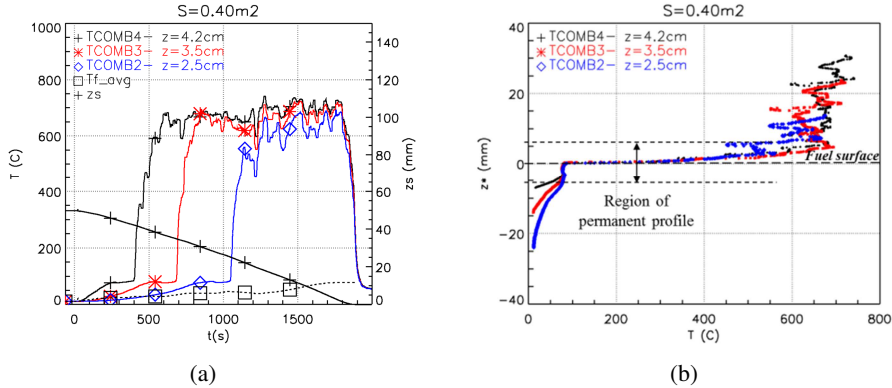


Fig. 6. (a) Time variation of temperature within the liquid and the gas phase and (b) corresponding vertical temperature profile during the steady phase where $z_p - z_s = 0$ corresponds to the fuel surface (PRS_SI_S8 test, ethanol, $S = 0.4 \text{ m}^2$).

Three temperature profiles, $T(t)$ versus $z^*(t)$ are computed during the period of time of quasi steady burning (here $t = [100, 1200]$ s) for each of the three thermocouples and are presented in Fig. 6 (b).

The profiles show similar behavior and three typical regions are identified. A first region of progressive increase of temperature from the bottom of the pan up to a position a few millimeters below the fuel surface, a second region of constant temperature (the boiling temperature) below the fuel surface and then a third region above the fuel surface characterized by a typical boundary layer profile and a strong temperature gradient near the surface. It must be noted that each profile contains points that are measured at different times and therefore they cannot be considered as a spatial temperature profile at a given time unless the phenomenon is steady and not transient which is not the case here.

However, the profiles analysis shows an important feature. There is a reduced part of the profile of a few millimeters from both sides of the fuel surface (in the region $z^*(t) = [-6; +6] \text{ mm}$) where the three curves are identical, whichever the thermocouple. This feature means that the temperature profiles in this reduced region are not time dependent (during the period considered here, $t = [100, 1200]$ s) and therefore can be considered as a spatial vertical profile. This protocol for determining the vertical temperature profile from fixed single thermocouples is only valid in the vicinity of the fuel surface where the profile is not affected by the transient behavior of the experiment. The other parts of the profiles, below the upper layer and far above the fuel surface, vary significantly between thermocouples and therefore cannot be considered for representing the average vertical temperature.

It is worth noting that the temperature measurement with thermocouples may be affected by two effects, the response time and the thermal radiation coming from the flame. The large response time of the 1.5 mm diameter thermocouple (several seconds) contributes to an underestimate of the real fluid temperature, whereas the thermal radiation leads to an overestimate. Due to these opposite effects, the two factors may cancel each other. Nevertheless, a reliable correction of the measured profiles is a difficult task due to the large number of input parameters. As a first approximation, the maximum error is estimated to be $\pm 25^\circ\text{C}$ for these experiments.

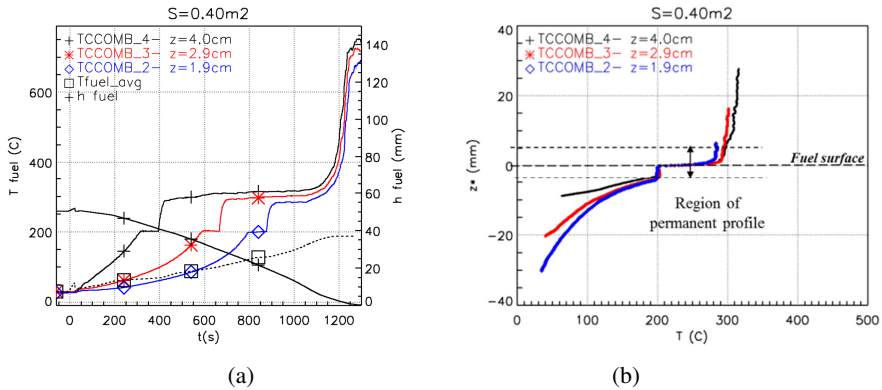


Fig. 7. (a) Time variation of temperature within the liquid and the gas phase and (b) corresponding vertical temperature profile during the steady phase (PRS_SI_S4 test, TPH, $S=0.4\text{ m}^2$).

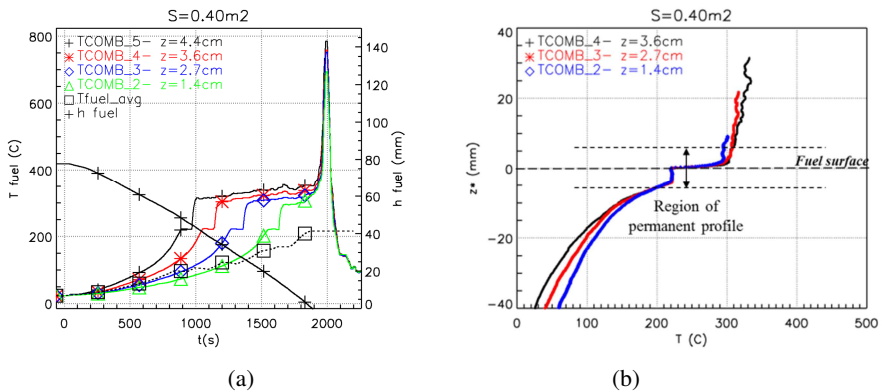


Fig. 8. (a) Time variation of temperature within the liquid and the gas phase and (b) corresponding vertical temperature profile during the steady phase (PR3_S3S_S1 test, Dodecane, $S=0.4\text{ m}^2$).

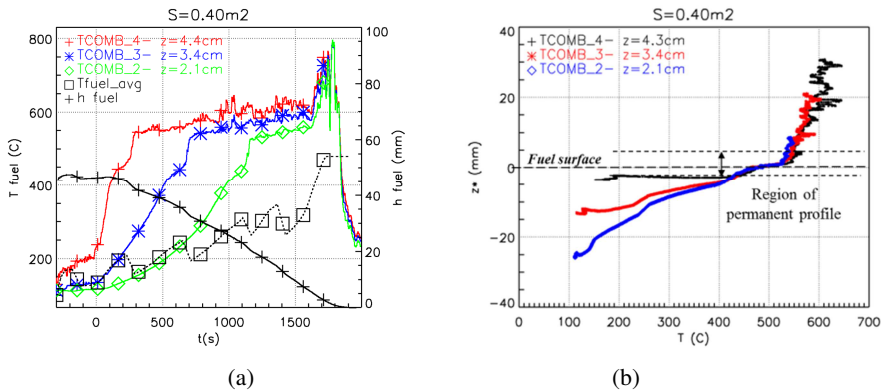


Fig. 9. (a) Time variation of temperature within the liquid and the gas phase and (b) corresponding vertical temperature profile during the steady phase (PR2_FESS_S12 test, Lubricant oil, $S=0.4\text{ m}^2$).

Similar results are obtained for other fuels as presented in Fig. 7 to Fig. 9. In the same way as for the ethanol experiment, there is a region of a few millimeters below and above the fuel surface where the temperature profiles given by the three thermocouples are identical and thus independent of the transient behavior of the experiment. This result obtained with the other fuels confirms the existence of a limited region of the temperature profile, here $[-6; 6]$ mm from both sides of the fuel

surface, unaffected by the transient behavior of the experiment. This behavior is also observed for the other pool sizes. A particular feature of this protocol is the high spatial resolution characterizing these profiles. Indeed, the spatial resolution is given by the relation $dz = \dot{m}_f'' / \rho(T) / f_{acq}$. With an acquisition frequency f_{acq} of 1 Hz for the present experiment, a mass loss rate per unit of area of about $30 \text{ g/m}^2/\text{s}$ and a density of about 800 kg/m^3 , it leads to a spatial resolution of about $4 \cdot 10^{-2} \text{ mm}$.

In order to get one temperature profile per experiment, a mean is computed from the three profiles and the result is presented in Fig. 10 and Fig. 11 for the four fuels in the limited region $z^* = [-6; 6] \text{ mm}$ from both sides of the fuel surface.

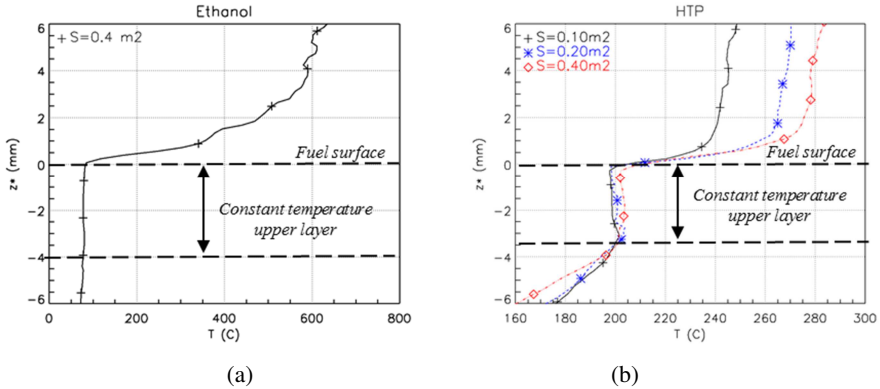


Fig. 10. Vertical temperature profiles (a) for Ethanol, (b) for HTP fuel for various pool sizes.

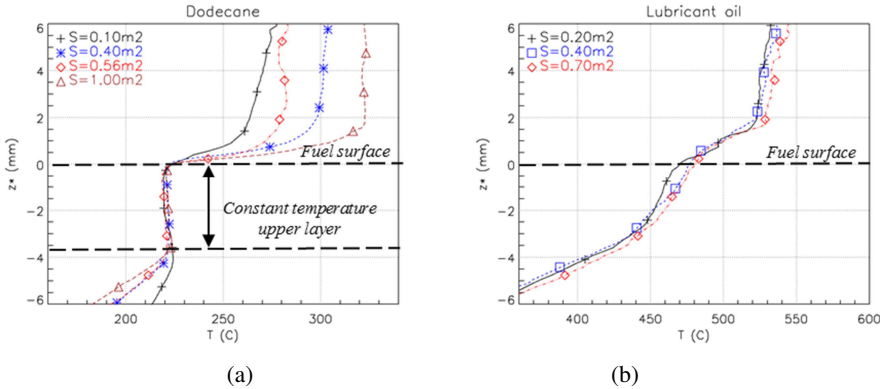


Fig. 11. Vertical temperature profiles for various pool sizes (a) for Dodecane, (b) for lubricant oil.

Ethanol, HTP and Dodecane fuels show the same typical profile with an upper layer in which the temperature is constant and equal to the boiling temperature. The values obtained experimentally from an average of the temperatures in the layer are about 80°C , 200°C and 220°C for Ethanol, HTP and Dodecane, respectively, and correspond to the values expected from the literature (cf. Table 2). The thickness of this layer is measured graphically and is about 4 mm as indicated in the figures and is constant whatever the fuel type and the pool size, in the range considered in this study. For some experiments, a hot spot of temperature is observed on the lower side of this upper layer. This phenomenon of upper layer at boiling temperature has already been reported in the literature in the 60s [12] and also more recently [11].

The existence of the upper layer results from a competition between the radiative heat absorbed within the first millimeters of the liquid and the amount of latent heat required to heat up the liquid up to the boiling temperature. If the boiling temperature is low, it is likely that a thin layer at boiling

temperature will be formed. However, this behavior is not systematically observed. For lubricant oil fuel, Fig. 11 (b), no upper layer at constant boiling temperature has been reported due to the high level of boiling temperature (about 480°C). However, for this fuel, the region a few millimeters below the surface shows also a special behavior with a change in the vertical temperature gradient dT/dz . The lack of upper layer at constant boiling temperature is explained by the high level of boiling temperature in comparison to the amount of radiative heat absorbed by the liquid fuel. The occurrence of this constant temperature upper layer is therefore not systematic and depends mainly on the fuel properties and possibly on the pool dimension. For higher pool sizes, the radiative heat flux can be more important and will favor the occurrence of the upper layer.

The analysis of the temperature profiles in the gas phase gives also information about convective heat transfer at the fuel surface that is characterized by a significant temperature gradient within a few millimeters. The highest gradient and therefore highest convective heat flux are observed for the ethanol pool fire. HTP and Dodecane fuels show similar behavior and lubricant oil fuel gives the lowest gradient. Figure 12 illustrates this quantitative comparison for a given pool area.

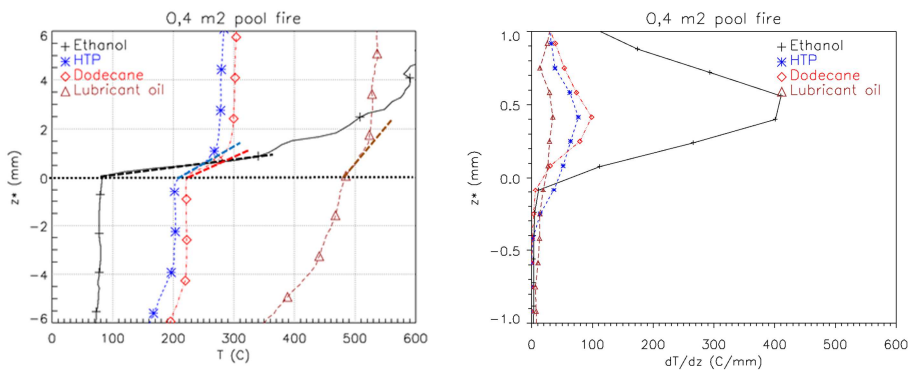


Fig. 12. (a) Vertical temperature profiles in the vicinity of the fuel surface for 0.4 m² pool fire for four fuels (b) corresponding spatial derivative dT/dz .

The effect of the pool size is different according to the fuel as illustrated in Fig. 10 and Fig. 12. For HTP and Dodecane fuels, the increase of the pool size contributes to an increase in the convective heat transfers. For lubricant oil fuel, no effect of the pool size is reported in the range considered (0.2-0.7) m². An explanation of this result is attributed to the level of fuel mass loss rate per unit area. In the range of pool sizes considered, the mass loss rate per unit area varies for lubricant oil fuel very little in comparison to HTP or Dodecane fuel. The measurements of the temperature profile in the thermal boundary layer may also give access to the convective heat transfer coefficient formulated as $h \sim \lambda/\delta$, with λ the thermal conductivity of the gaseous fuel and δ the thickness of the viscous layer in which the temperature gradient is constant and the heat transfer takes only place by conduction. The thermal conductivity of gaseous fuel at boiling temperature is in the range 25-40 mW/(m·K). Assessment of the viscous layer thickness is determined from the temperature profiles, considering that this layer is characterized by a maximum and constant gradient. An example of the gradient of temperature is given in Fig.12 (b). Although it remains difficult to extract an accurate value from the present measurements, in a first preliminary approach, a rough estimation of this thickness is about half of a millimeter or lower. These estimates of the thermal conductivity and the viscous layer thickness lead to a convective heat transfer coefficient of the order of 50-80 W/(m²·K). This order of magnitude is much larger than indirect measurement deduced from the energy balance approach, for instance 6 W/(m²·K) by [2]. This difference may suggest that the methodology may have an influence: The energy balance approach proposes a deduction of the convective contribution whereas the present work permits a direct calculation. Further

investigations should be performed to determine the value of the heat transfer coefficient with better accuracy.

CONCLUSION

This study has investigated heat and mass transfer at the liquid fuel surface in pool fires. Temperature profiles in the vicinity of the fuel surface in both liquid and gas phases have been presented from pool fire tests, performed in open atmosphere with various pool dimensions and liquid fuels (Ethanol, Dodecane, Hydrogenated TetraPropylene and Lubricant oil). A simple protocol based on the measurement of temperature with thermocouples gives high spatial discretization temperature profiles. The results indicate that an upper layer below the fuel surface at constant temperature exists for Ethanol, Dodecane and Hydrogenated TetraPropylene fuels. The temperature profiles allow an assessment of the convective heat transfer at the fuel surface. These results are new data and can be valuable inputs for validation of fuel evaporation models developed for pool fires.

REFERENCES

- [1] A. Hamins, T. Kashiwagi, R. Burch, Characteristics of pool fire burning, Fire Resistance of Industrial fluids, June 20, 1995, Indianapolis, In: Proceedings ASTM STP 1284, Philadelphia P. A. Totten, G. E., Reichel J. (Ed.), 1996.
- [2] L. Orloff, J. de Ris, Froude Modeling of Pool Fires, Proc. Combust. Inst. 19 (1982) 885-895.
- [3] A. Hamins, J. Fischer, T. Kashiwagi, M.E. Klassen, J.P. Gore, Heat feedback to the fuel surface in pool fires, Combust. Sci. Technol. 97 (1994) 37-62.
- [4] V. Babrauskas, Heat release rates, in: SFPE Handbook of Fire Protection Engineering, 3rd ed. NFPA Quincy, MA, 2002.
- [5] S. Hostikka, K. McGrattan, A. Hamins, Numerical modeling of pool fire using large eddy simulation and finite volume method for radiation, In: Fire safety Science – Proceeding of the 7th International Symposium of IAFSS, 2002, pp. 383-394.
- [6] H. Pretrel, S. Suard, L. Audouin, Experimental and numerical study of low frequency oscillatory behaviour of a large-scale hydrocarbon pool fire in a mechanically ventilated compartment, Fire Saf. J. 83 (2016) 38-53.
- [7] T. Sikanen, S. Hostikka, Modeling and simulation of liquid pool fires with in-depth radiation absorption and heat transfer, Fire Saf. J. 80 (2016) 95-109.
- [8] A. Nakakuki, Heat transfer in pool fires at certain small lip height, Combust. Flame 131 (2002) 259-272.
- [9] A. Vali, D. Nobes, L. W. Kostiuik, Characterization of flow field within the liquid phase of a small pool fire using particle image velocimetry technique, Exp. Thermal Fluid Sci. 75 (2016) 228-234.
- [10] A. Vali, D. Nobes, L. W. Kostiuik, Effects of altering the liquid phase boundary conditions of methanol pool fires, Exp. Thermal Fluid Sci. 44 (2013) 786-791.
- [11] A. Vali, D. Nobes, L. W. Kostiuik, Fluid motion and energy transfer within burning liquid fuel pools of various thicknesses, Combust. Flame 162 (2015) 1477-1488.
- [12] V.I. Blinov, G. Khudyakov, Diffusion burning of liquids, In: U.S. Army Translation, NTIS No. AD296762, 1961.
- [13] J.M. Suo-Anttila, T.K. Blanchat, A.J. Ricks, A.L. Brown, Characterization of thermal radiation spectra in 2m pool fires, Proc. Combust. Inst. 32 (2009) 2567-2574.
- [14] J. Zhao, H. Huang, G. Jomaas, M. Zhong, R. Yang, Experimental study of the burning behaviors of thin-layer pool fires, Combust. Flame 193 (2018) 327-334.
- [15] T. Beji, B. Merci, Development of a numerical model for liquid pool evaporation, Fire Saf. J. 102 (2018) 48-58.